U.S. Department
of Transportation
Federal Railroad
Administration

Office of Research,
Development and Technology
Washington, DC 20590

Laser Triangulation and Deep Neural Networks for Rail Safety Inspections — Phase 2: Framework for Isolating and Reporting Track Changes

DOT/FRA/ORD-26/03

Final Report | April 2026

REPORT DOCUMENTATION PAGE

Form Approved
OMB No. 0704-0188

1. REPORT DATE *(DD-MM-YYYY)*	**2. REPORT TYPE**	**3. DATES COVERED** *(From - To)*
7 April 2026	Technical Report	October 2020 – December 2023

4. TITLE AND SUBTITLE

Laser Triangulation and Deep Neural Networks for Rail Safety Inspections — Phase 2: Framework for Isolating and Reporting Track Changes

5a. CONTRACT NUMBER
693JJ6-20-C-000035

5b. GRANT NUMBER

5c. PROGRAM ELEMENT NUMBER

6. AUTHOR(S)
Arthur de O. Lima, ORCID: 0000-0002-9642-2931
J. Riley Edwards, ORCID: 0000-0001-7112-0956
Ian Germoglio Barbosa, ORCID: 0009-0006-8785-2055
Sadaf Shafie Z. A., ORCID: 0009-0006-1306-8487
Paula Palma, ORCID: 0009-0006-8335-5975
Marcus S. Dersch, ORCID: 0000-0001-9262-3480

5d. PROJECT NUMBER

5e. TASK NUMBER

5f. WORK UNIT NUMBER

7. PERFORMING ORGANIZATION NAME(S) AND ADDRESS(ES)
University of Illinois at Urbana-Champaign
506 S. Wright St.
Urbana, IL 61801-3620

8. PERFORMING ORGANIZATION REPORT NUMBER

N/A

9. SPONSORING/MONITORING AGENCY NAME(S) AND ADDRESS(ES)
U.S. Department of Transportation
Federal Railroad Administration
Office of Research, Development, and Technology
1200 New Jersey Avenue, SE
Washington, DC 20590

10. SPONSOR/MONITOR'S ACRONYM(S)

11. SPONSOR/MONITOR'S REPORT NUMBER(S)
DOT/FRA/ORD-26/03

12. DISTRIBUTION/AVAILABILITY STATEMENT
This document is available to the public through the FRA website.

13. SUPPLEMENTARY NOTES
COR: Cameron Stuart

14. ABSTRACT
This research builds upon previous FRA-funded studies using the LRAIL 3D laser triangulation scanning system and Deep Convolutional Neural Networks (DCNNs) to identify track health attributes. The focus lies on developing technology-agnostic methodologies for processing LRAIL data, catering to diverse end-users in the railway sector. At the component level, a track component health index (TCHI) is introduced, offering a numerical evaluation of track health based on component conditions. Specific indexes for ballast, crossties, and fasteners are combined into a global TCHI, providing a holistic understanding of rail superstructure condition. From a system level, the research also introduces the track strength index (TSI) to numerically assess track buckling resistance. Machine vision-based inspections prove valuable for infrastructure owners, aiding in condition detection and tracking. This approach offers a holistic and quantifiable understanding of track health and strength, enhancing maintenance strategies and overall railway safety. Visualization of data supports decision-makers in prioritizing maintenance, potentially reducing the risk of track-caused derailments.

15. SUBJECT TERMS
3D laser triangulation, artificial intelligence, AI, deep convolutional neural networks, algorithms, change detection, safety, operational efficiency, inspection, track buckling, lateral resistance, track lateral strength

16. SECURITY CLASSIFICATION OF:			**17. LIMITATION OF ABSTRACT**	**18. NUMBER OF PAGES**	**19a. NAME OF RESPONSIBLE PERSON**
a. REPORT	**b. ABSTRACT**	**c. THIS PAGE**		35	**19b. TELEPHONE NUMBER** *(Include area code)*

Standard Form 298 (Rev. 8/98)
Prescribed by ANSI Std. Z39.18

METRIC/ENGLISH CONVERSION FACTORS

ENGLISH TO METRIC	METRIC TO ENGLISH
LENGTH (APPROXIMATE)	**LENGTH (APPROXIMATE)**
1 inch (in) = 2.5 centimeters (cm)	1 millimeter (mm) = 0.04 inch (in)
1 foot (ft) = 30 centimeters (cm)	1 centimeter (cm) = 0.4 inch (in)
1 yard (yd) = 0.9 meter (m)	1 meter (m) = 3.3 feet (ft)
1 mile (mi) = 1.6 kilometers (km)	1 meter (m) = 1.1 yards (yd)
	1 kilometer (km) = 0.6 mile (mi)
AREA (APPROXIMATE)	**AREA (APPROXIMATE)**
1 square inch (sq in, in^2) = 6.5 square centimeters (cm^2)	1 square centimeter (cm^2) = 0.16 square inch (sq in, in^2)
1 square foot (sq ft, ft^2) = 0.09 square meter (m^2)	1 square meter (m^2) = 1.2 square yards (sq yd, yd^2)
1 square yard (sq yd, yd^2) = 0.8 square meter (m^2)	1 square kilometer (km^2) = 0.4 square mile (sq mi, mi^2)
1 square mile (sq mi, mi^2) = 2.6 square kilometers (km^2)	10,000 square meters (m^2) = 1 hectare (ha) = 2.5 acres
1 acre = 0.4 hectare (he) = 4,000 square meters (m^2)	
MASS - WEIGHT (APPROXIMATE)	**MASS - WEIGHT (APPROXIMATE)**
1 ounce (oz) = 28 grams (gm)	1 gram (gm) = 0.036 ounce (oz)
1 pound (lb) = 0.45 kilogram (kg)	1 kilogram (kg) = 2.2 pounds (lb)
1 short ton = 2,000 pounds (lb) = 0.9 tonne (t)	1 tonne (t) = 1,000 kilograms (kg) = 1.1 short tons
VOLUME (APPROXIMATE)	**VOLUME (APPROXIMATE)**
1 teaspoon (tsp) = 5 milliliters (ml)	1 milliliter (ml) = 0.03 fluid ounce (fl oz)
1 tablespoon (tbsp) = 15 milliliters (ml)	1 liter (l) = 2.1 pints (pt)
1 fluid ounce (fl oz) = 30 milliliters (ml)	1 liter (l) = 1.06 quarts (qt)
1 cup (c) = 0.24 liter (l)	1 liter (l) = 0.26 gallon (gal)
1 pint (pt) = 0.47 liter (l)	
1 quart (qt) = 0.96 liter (l)	
1 gallon (gal) = 3.8 liters (l)	
1 cubic foot (cu ft, ft^3) = 0.03 cubic meter (m^3)	1 cubic meter (m^3) = 36 cubic feet (cu ft, ft^3)
1 cubic yard (cu yd, yd^3) = 0.76 cubic meter (m^3)	1 cubic meter (m^3) = 1.3 cubic yards (cu yd, yd^3)
TEMPERATURE (EXACT)	**TEMPERATURE (EXACT)**
[(x-32)(5/9)] °F = y °C	[(9/5) y + 32] °C = x °F

QUICK INCH - CENTIMETER LENGTH CONVERSION

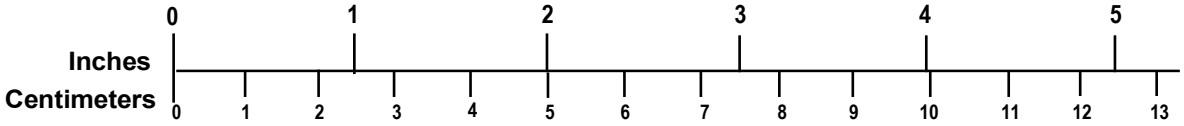

QUICK FAHRENHEIT - CELSIUS TEMPERATURE CONVERSIO

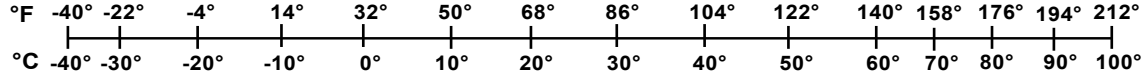

For more exact and or other conversion factors, see NIST Miscellaneous Publication 286, Units of Weights and Measures. Price $2.50 SD Catalog No. C13 10286

Updated 6/17/98

Contents

Illustrations

Tables

Executive Summary

The research project detailed in this report builds on previous FRA-funded research using a 3D laser triangulation scanning system (LR*AI*L) and deep convolutional neural networks to identify various attributes related to track health. This project focused on the development of methodologies to consume Pavemetrics' LR*AI*L data outputs to better estimate and understand the condition and strength of the track system and its components. The methodology is designed to be technology-agnostic and thus compatible with data from other inspection systems with similar track component conditions. The depth and breadth of the data collected by LR*AI*L present an opportunity to process and present information to a variety of end users within the railway organizational structure. Distinct end-users have unique use cases for such data and need to consume it at a different level of specificity.

At the component level, University of Illinois at Urbana-Champaign (UIUC) researchers developed a track component health index (TCHI) to provide an objective, numerical quantification of the track health based on the current condition of its components. UIUC developed health indices for ballast, crossties, and fasteners. They combined and weighted them into a global TCHI value. The TCHI methodology provides an analytical and numerical way to assess track component health and holistically understand rail superstructure condition. These data can augment the track inspector's findings and serve other stakeholders in the railway organization interested in monitoring and comparing the health state of the track as it changes over time.

This research also explored the potential of these outputs to aid in rail neutral temperature (RNT) management and track buckle risk mitigation through the development of a metric that facilitates the assessment of lateral and longitudinal track strength. The track strength index (TSI) numerically quantifies track buckling resistance at a system level. The TSI combines both the in-situ condition of track components and track geometry data by giving higher weights to factors that have been demonstrated to have a larger influence on track buckling strength.

Combined, these indexes can provide a more complete understanding of both absolute and relative track health and strength. Machine vision-based track inspections add value to the track inspection activity through the highly precise detection and tracking of condition changes over time and tonnage. The visualization of data assists decision-makers in prioritizing and optimizing maintenance strategies, ultimately mitigating the risk of track-caused derailments.

Further refinement of TCHI and its sub-indexes presented here can be achieved by employing owner-specific business rules or engineering requirements resulting in a more customized and specific presentation of these data for railroad operators. In addition, future work for TSI may focus on developing a more comprehensive model or index that considers the demand side of the track buckle equation by incorporating rail temperature, its deviation from RNT, and forces induced by trains accelerating and braking.

1. Introduction

This project continues earlier track condition change detection research funded by the Federal Railroad Administration (FRA) that was conducted by the Rail Transportation Engineering Center (RailTEC) of the University of Illinois at Urbana-Champaign (UIUC) and Pavemetrics (Fox-Ivey et al., 2020a; Fox-Ivey et al., 2020b; Harrington et al., 2023). UIUC led this research project between October 2020 and December 2023.

1.1 Background

In its role as a regulatory body, FRA specifies track inspection intervals and the primary duties and qualifications of a certified track inspector (FRA, 2020). Technology advances, especially in machine vision, offer the potential to augment these processes with highly precise and actionable information about the condition of the track infrastructure. The rail industry is adopting machine vision technologies to improve awareness of the effects of time and tonnage on the track structure.

A variety of advances in rail engineering technologies have been developed and deployed over the past decade, including vehicle-track interaction (VTI) systems for track condition assessment (Tesic et al., 2018) and non-destructive methods to determine rail component condition (Clark, 2004; Rudy et al., 2006; Wu et al., 2021; Evani et al., 2021). These, along with other new and emerging technologies, provide the rail industry with an opportunity to improve safety and optimize maintenance strategies to produce a network that is safer, more reliable, and more efficient. At the same time, there has been an upward trend in both rail traffic volumes and railcar axle loadings (Sogin et al., 2012) which place increasing demand on the track infrastructure system and its components The rail industry may be able to leverage new methods and technologies to further reduce track-caused derailments beyond the steady state condition of 0.85 derailments per million-train-miles over the past decade (Association of American Railroads, 2020). From a financial perspective, delays caused by maintenance activities or service interruptions due to a lack of maintenance influence track availability for revenue generation through train movements. This affects numerous stakeholders within the global supply chain, including railroads, shippers, and the public (Lovett et al., 2015).

Improvements in rail transportation safety and derailment reduction have been ongoing priorities for both the rail industry and FRA, reflected in a 39 percent reduction in freight train derailments between 2005 and 2017 (Wang and Barkan, 2017). With increasing demands on most primary rail corridors in the U.S., Class I operators are adopting new technologies for inspection and maintenance. The introduction of autonomous inspection systems leveraging 3D laser triangulation and deep convolutional neural networks (DCNNs) can provide a solution to inventory track and optimize rail infrastructure assets (Fox-Ivey et al., 2020b; Harrington et al., 2022). When 3D laser technology is paired with properly trained DCNNs, they can reliably detect a variety of track components and conditions (Harrington et al., 2022). The research summarized in this report used a 3D laser triangulation scanning system (LR*AI*L) which combines pulsed, high-power, invisible laser line projectors and synchronized cameras to capture a high-resolution intensity image and range profile of rail track (Fox-Ivey et al., 2020a). The LR*AI*L system is capable of inspecting tracks at typical mainline speeds, and data are collected at either one- or two-mm intervals. Data are then combined into range (3D laser) and intensity (2D line scan) images that are two meters in length (Figure 1).

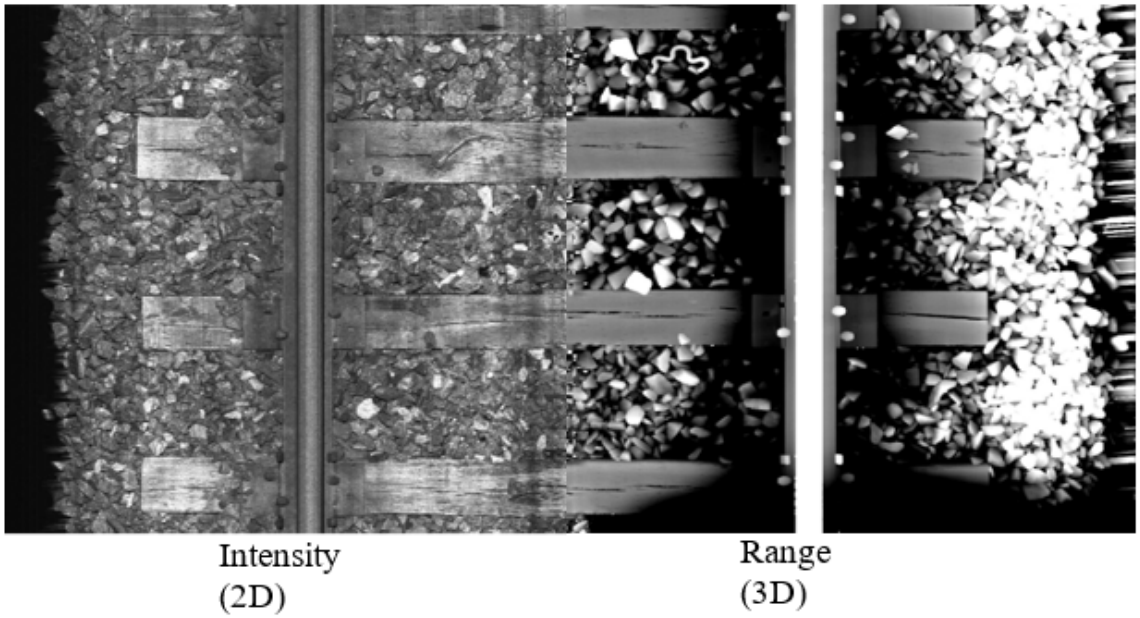

Figure 1. Example LR*AI*L intensity (left) and range (right) output images

These images are subsequently evaluated by DCNNs, which identify various attributes related to the health of the track system and its components. The DCNNs leveraged in this research demonstrated 98 percent precision after training (Harrington et al., 2022). This research also documented the development of a proposed methodology to report inspection data and established a benchmark for uniform representation of 3D laser scanning data using strip charts. When track components are analyzed as a collective system, the output provides a holistic view of the track condition and gives insight to future problems the track may experience. Consequently, this gives researchers a wide range of analysis possibilities and data use cases, and targeted reports specific to different end-user's needs and job function can be generated.

1.2 Objectives

The main objective of this research study was to develop new methodologies to consume outputs from the LR*AI*L inspections system to produce novel indices that provide a more complete assessment of the track health.

1.3 Overall Approach

The depth and breadth of the data collected by LR*AI*L provide an opportunity to process and present information to a variety of end users within the railway organizational structure. Distinct end-users have unique use cases for such data and need to consume it at different levels of specificity. The combination of different LR*AI*L outputs can generate insight for track inspectors, maintenance planners, and senior management. Figure 2 identifies proposed reporting levels and the associated primary and secondary end-users for each analysis output, along with the major analysis that can be performed using LR*AI*L data.

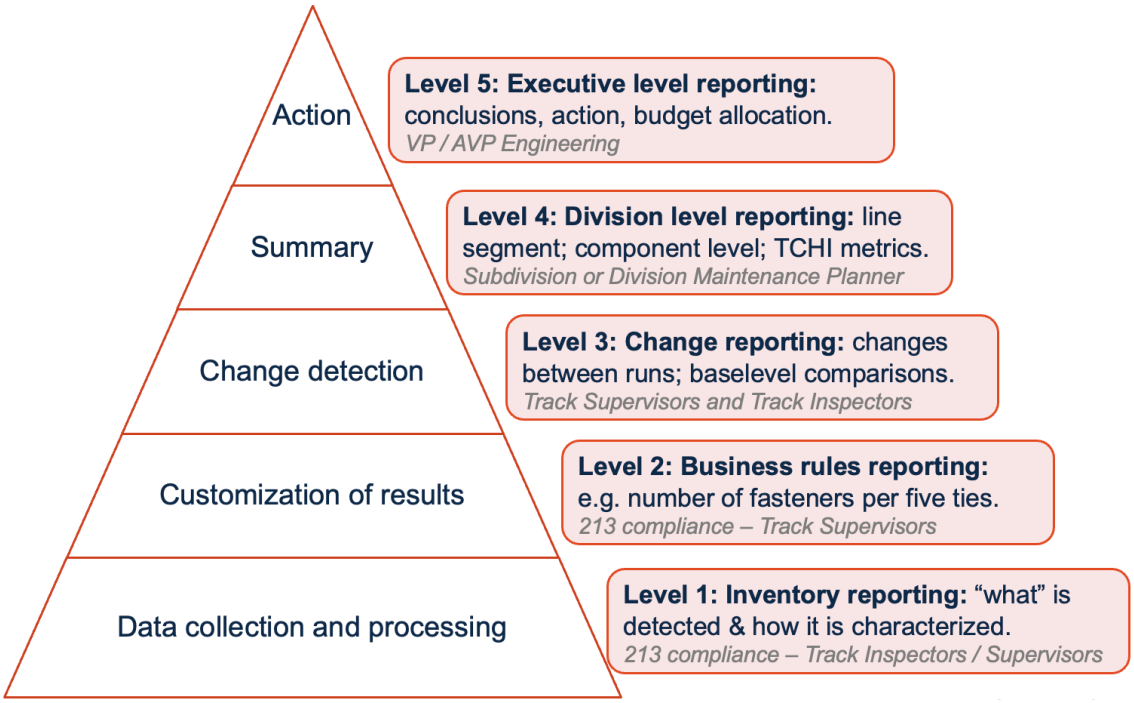

LR*AI*L Output / Data Visualization Method	Pyramid Level (Figure 1)	Track Inspector	Track Supervisor	Maintenance Planner
Track Changes Over Time	Level 3	P	P	
Inventory Chart	Level 1		P	P
Real-time Track Change Visuals	Levels 2 and 3	P	S	
Track Component Health Index	Level 4		P	P
Component Rate of Change	Level 3	S	P	S
Subdivision TCHI Metrics	Level 4		S	P
Subdivision Metrics Over Time	Level 4		S	P

P = Primary User; S = Secondary User

Figure 2. Data analysis and utilization pyramid and example data outputs for end-users

Regulations for U.S. track conditions are described in 49 C.F.R. § 213 – Track Safety Standards (FRA, 2022). The FRA Track and Rail and Infrastructure Integrity Compliance Manual (FRA, 2017), hereafter referred to as the "Compliance Manual", provides additional interpretation and commentary of 49 CFR § 213. In addition, railroads maintain their own (generally more restrictive) set of rules that are commonly referred to as "engineering instructions" (BNSF Railway, 2018; Union Pacific Railroad, 2019) to guide field personnel who construct and maintain track. Engineering instructions typically contain information about track component selection, patterns, sizes, and quantities. This research created numerical and objective condition thresholds for each component by leveraging these documents, along with relevant peer-reviewed literature and other documentation of research. These rules and thresholds can be adapted to meet the needs of different end-users.

Trained DCNNs process LR*AI*L data in a manner that classifies component location, presence or absence, and condition in comma separated values (CSV) file format. The magnitude of available data varies based on the inspected component type and density. The output file reports

track components, track geometry, and crosstie-based information, along with geographical information and track stationing. At the base level of the pyramid, Level 1, (Figure 2) the direct output of the DCNNs provides an inventory of components. Subsequently, as a part of Level 2 analysis, business rules are applied for fasteners, ballast, and crossties. Indices are calculated based on the number of components present or, in the case of ballast, the relative height to the top of the crosstie and range from 0 (worst condition) to 10 (best condition). Next, the process combines individual component indices and assigned weights to each of them, leading to the development of the track component health index (TCHI).

This research also explored the potential for LR*AI*L data to address one of the risks of continuous welded rail (CWR), track buckling. Lateral track movement may occur and potentially result in buckles under conditions of compressive thermal stresses resulting from rail temperature exceeding the temperature at which the axial stress in the rail is zero, referred to as the rail neutral temperature (RNT) or stress-free temperature (Belding et al., 2023). Buckling occurs when the rail axial forces due to thermal gradient and rolling stock braking or acceleration exceed the resisting forces provided from the track structure (Van, 1996; Hasan, 2021). While numerous studies have focused on track buckling mechanics and prevention, a practical and objective method is still needed to assess resistance to buckling in the field.

Conceptually, ensuring the track has sufficient strength to resist induced lateral demand results in a stable track that should not buckle. To further improve track safety by reducing the occurrence of track buckle-caused derailments, UIUC developed a metric that facilitates the assessment of track buckle strength using quantifiable parameters. The track strength index (TSI) numerically quantifies track buckling resistance at a system level. The TSI combines both the in-situ condition of track components and track geometry data by giving higher weights to those factors that have been demonstrated to have a larger influence on track buckling strength. The TSI is objective, which enables comparison over time and tonnage and provides quantitative insights into track strength improvement and deterioration, the latter of which may require maintenance intervention to ensure track adequacy.

Both TCHI and TSI outputs can be reported and displayed graphically using strip charts as well as histograms, bar charts, and maps. These visualization methods can be customized based on the function of the employee consuming the data (e.g., track inspector vs. division maintenance planner) to maximize track condition data and information utility for their respective needs.

While the use of indexes to objectively quantify track health in a continuous manner along the track is not new, the development and application of indexes to assess track component health using imaged-based sensing data is novel. Examples of other indexes that have been developed to assess the track structure include the FRA Track Quality Index (Soleimanmeigouni et al., 2020), U.S. Track Roughness Index (Ebersohn and Ruppert, 1998), Swedish National Railway Q Index (Andersson, 2002), Chinese Track Quality Index (Liu et al., 2015), Ballast Fouling Index (Sadeghi et al., 2018), and the Track Structural Index (Sadeghi and Askarinejad, 2010). These track superstructure-related indices focus on the evaluation and presentation of track geometry data and tend to overlook the assessment of components. Furthermore, no index currently combines geometric parameters with railway component condition levels or quantifies track buckle resistance.

1.4 Scope

This report summarizes the development of methodologies to consume LR*AI*L data outputs to better estimate and understand the condition and strength of the track system and its components. The methodology is designed to be technology-agnostic and thus compatible with data from other inspection systems with similar track component conditions. The research developed two novel indexes related to track health, the TCHI and the TSI. The scope of this report includes a description of the data used, methodologies, and assumptions embedded into each index, data analysis methods and calculations, and example results for each index.

1.5 Organization of the Report

This report has four sections. Section 2 provides a detailed review of TCHI development and example results. Section 3 provides a detailed review of TSI development and example results. Finally, Section 4 provides conclusions and recommendations for future work.

2. TCHI Development

The following sections discuss the development of the TCHI and its sub-indexes. The indexes are generated by obtaining linear LR*AI*L data, processing data using DCNNs, and then distilling data into clusters and other metrics for visualization via bar charts, GIS-based maps, and strip charts.

2.1 Initial Field Site and Data Collection

Under a prior contract, UIUC used the High Tonnage Loop (HTL) at FRA's Transportation Technology Center (TTC) in Pueblo, CO as a proof-of-concept test site. The HTL provided a rich test bed with many component varieties and the ability to collect repeated scans of data under rapid tonnage accumulation in a very short amount of time given the concurrent operation of the heavy axle load test train as a part of the Facility for Accelerated Service Testing operations. An FRA technical report by Harrington et al. (2023) describes the development of the DCNN through the collection and use of training data. Additionally, Harrington et al. (2022) developed a proposed methodology to report inspection data and established a benchmark for uniform representation of 3D laser scanning data using strip charts.

For TCHI validation purposes, researchers used a subsection of the HTL at TTC known as Section 3. They chose this 2,800-ft-long section due to the quality and completeness of the data available. The track construction contained both concrete and timber crossties, enabling researchers to validate the premises and calculations for TCHI. Researchers first conducted a ground truth survey, visually checking the images and comparing findings to the results output by the DCNNs to data collected by human inspectors on the ground (Harrington et al., 2022).

2.2 Default Thresholds (Business Rules)

Railway track components function as a system (Hay, 1982; Kerr, 2003), and each constituent component must be analyzed to develop composite indexes related to track structural health. This section details the selection of the default compliance and safety thresholds for cut spikes, screw spikes, elastic fasteners, anchors, crossties, and the ballast section. These were selected based on multiple criteria, inspection distances, and documents. Taken as a whole, the compliance thresholds are based on engineering instructions from Class I Railroads or compliance thresholds described in the FRA Track Safety Standards (FRA, 2011) and the safety thresholds are from CFR § 213 (FRA, 2011).

2.2.1 Cut and Screw Spikes

Cut spikes are the most common rail fastener used on North American railroads (Gao et al., 2020). Determining maintenance and safety rules for spikes is challenging due to the variety of spiking patterns adopted by railroads and the lack of research quantifying the influence of missing or broken spikes on track performance. Independent of the specific spiking pattern, tie plates are expected to be installed with at least two spikes (Union Pacific Railroad, 2019). Thus, any condition of less than two spikes per plate is classified as exceeding the safety threshold. An industry expert with experience in the use of cut and screw spikes at a Class I railroad provided inputs for the development of business rules related to spikes. UIUC researchers determined that a rate of 20 percent for missing spikes would be used as a baseline maintenance threshold.

The safety threshold for missing spikes should not be stricter than what is applied to broken crossties (Section 2.2.4), as experts agree that a single missing spike is less critical than one defective crosstie containing four or more spikes. However, raising the missing spike threshold beyond 40 percent (the number used for crossties) does not seem adequate for two reasons. First, there are no experimental data to inform such an increase. Second, spikes may be present but may be ineffective (e.g., broken within crosstie) and thus cannot be detected in a visual or laser-based inspection (Dersch et al., 2019). Thus, the authors selected 40 percent as the safety threshold for missing spikes. In addition, researchers selected a moving inspection window of 25 crossties for cut spikes. This closely corresponds to the common FRA inspection distance of one rail length (39 ft; FRA, 2017) considering typical timber crosstie spacing of 19.5 in. This inspection window was also chosen to facilitate efficient calculations since the data are output on a crosstie-by-crosstie basis.

2.2.2 Elastic Fasteners

Elastic fasteners apply a vertical clamping force, or toe load, to restrain the rail from moving longitudinally relative to the crosstie (Hasap et al., 2018). They are primarily used with concrete crossties and, despite some relationship to cut spikes in their design function, installation method, and number per crosstie, their interaction with other components is quite different.

Researchers established the elastic fastener compliance threshold using 49 CFR §213, which states that "concrete crossties shall not be configured with less than two fasteners on the same rail" (FRA, 2011). Further, researchers also evaluated the threshold in light of results from a field study on the effects of missing or broken fasteners on gauge restraint of concrete crossties on Amtrak, which showed that three consecutive crossties with missing clips were needed to significantly reduce gauge restraint (Maal and Carr, 2011). UIUC selected a business rule threshold of 40 percent or more of crossties with at least one fastener missing and a safety threshold of 60 percent or more fasteners missing. All these criteria are evaluated within an inspection window of five crossties, based on the ranges proposed by Maal and Carr (2011).

2.2.3 Anchors

Anchors are responsible for resisting longitudinal rail movement (Ying Li et al., 2014) and are mostly used in timber crosstie track. Consequently, this rule is only considered in areas of timber crossties. Researchers selected the compliance threshold based on a Class I railroad's engineering instructions that every other crosstie should be box anchored. Due to the nature of this rule, the inspection window varies based on how many consecutive crossties have missing anchors. If the data show consecutively missing anchors, the size of the moving inspection window increases.

2.2.4 Crossties

The FRA compliance manual states that crossties are evaluated individually by the criteria outlined in its regulations (FRA, 2017). Crosstie effectiveness is inherently subjective and requires judgment in the application and interpretation of the regulations. Pavemetrics' internal data processing system that consumes LR*AI*L data gives a crosstie grading score. The software evaluates the dimensions of splits and cracks on the surface of the crossties and assigns an overall crosstie grade. The algorithm first classifies each crack into six different categories based

on depth, width, and length. It then combines the results of all cracks in a single crosstie and determines an overall condition based on surface area (Table 1 and Table 2).

Table 1. Crosstie crack classification methodology

Classification	Depth	Width	Length
Very severe	Crossties contain ballast materials	Crossties contain ballast materials	Crossties contain ballast materials
Severe	≥7/8”	≥2”	≥23 5/8”
Moderate	3/8” to ≥7/8”	1 1/4” to 2”	5 7/8” to 23 5/8”
Light	Not considered	3/8” to 7/8”	4” to 5 7/8”
Very Light	Not considered	1/4” to 1 1/4 “	Not considered
Unmarked	Not considered	<1/4”	Not considered

Table 2. Crosstie condition rating methodology

Rating	Numerical Value	Overall Crosstie Rating
Failed	3	More than 3.7% of crosstie surface containing very severe, severe, moderate, or light defects
Near Failure	2	Between 3.7% and 3.1% of crosstie surface containing very severe, severe, moderate, or light defects
Fair Condition	1	Between 3.1% and 2.6% of crosstie surface containing very severe, severe, moderate, or light defects
Good Condition	0	Any crosstie which does not fall into the 3 above categories

According to 49 CFR § 213.109 (FRA, 2011), each 39-ft (11.9 m) segment of track shall have a minimum number of crossties depending on the class of the track, geometry characteristics, and crosstie material (Table 3). By incorporating these parameters and requirements, researchers defined the safety limit as 40 percent of failed crossties or 70 percent of near-failure crossties, and the compliance limit as 25 percent of failed crossties or 50 percent of near-failed crossties in a 25-crosstie moving window.

Table 3. Minimum acceptable number of crossties in a 39-ft (11.9 m) track segment based on FRA track class

FRA Track Class	Numerical Value		Overall Crosstie Rating	
	19-in spacing	24-in spacing	19-in spacing	24-in spacing
Class 1	19 (79%)	14 (74%)	18 (75%)	13 (68%)
Class 2	16 (67%)	11 (58%)	15 (63%)	10 (53%)
Class 3	16 (67%)	11 (58%)	14 (58%)	9 (47%)
Classes 4 and 5	12 (50%)	7 (37%)	10 (42%)	5 (26%)

2.2.5 Ballast

The ballast is expected to transmit and distribute track loads to the subgrade, restrain track movement, and facilitate water drainage (Huang et al., 2009; Moaveni et al., 2016; Union Pacific Railroad, 2019). The ballast surface profile changes over time due to weather, interaction with other components, and train loading. Abrupt changes in ballast profile can negatively affect track performance.

Prior research relates the lack of lateral resistance to insufficient ballast, fouled ballast, or a combination of these factors (Khatibi et al., 2017a; Ngamkhanong et al., 2021). The LR*AI*L

system is limited to analyzing what is visible from the surface and reports ballast level as the absolute distance between a plane drawn between the top of both rails and the mean height of the ballast surface (Figure 3). The results are reported on a 1-m basis separately for crib, left shoulder, and right shoulder areas.

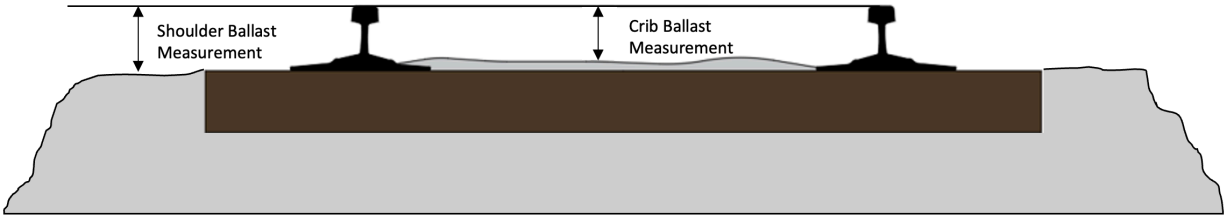

Figure 3. Ballast level measurement methodology

Each Class I railroad defines its design ballast section and profile specific to crosstie type, track use (e.g., mainline, siding, industrial), and degree of curvature. According to Union Pacific's engineering documents (Union Pacific Railroad, 2019), the ballast level should be even with the top of the crosstie. This requirement delineates the first compliance threshold for ballast when the height of the ballast is below the top of the crosstie.

Lower ballast levels reduce track structural capacity as demonstrated in results from various studies investigating different ballast levels and lateral resistance and their implication on safety (Khatibi et al., 2017a). However, other mechanisms influence the structural behavior of the ballast section (e.g., angularity of particles, gradation). UIUC established the safety limit as the point at which the ballast level decreases to below 50 percent of the crosstie height.

2.2.6 Business Rules Summary

A summary of the business rules introduced in the previous sub-sections can be found in Table 4.

Table 4. Summary of business rules developed by RailTEC

Component	Criteria	Inspection Window	Compliance Rule	Safety Rule
Cut and Screw Spikes	Presence	25 crossties	20% missing	40% missing
Elastic Fasteners	Presence	5 crossties	40% missing	60% missing
Anchors	Presence	Variable	Flagged when different from every other tie anchored	Flagged when different from every other tie anchored
Crossties	Grading	25 crossties	25% failed ties or 50% near failure	40% failed ties or 70% near failure
Ballast	Crib and shoulder level	10 meters	Less than top of crosstie surface	Less than 50% of crosstie height

2.3 Track Component Inventory

The first and lowest-level output is component inventory (Figure 2). This output provides a count of each component (e.g., crossties, fasteners, anchors, etc.; Figure 4a) and identifies the type of components (e.g., timber or concrete crosstie; Figure 4b). This information is useful when assessing the quantity of railroad infrastructure components. Capital planning teams can use this information to forecast future expenses and management teams can leverage it to see the overall

performance of track components and provide guidance on where more detailed track inspection may be needed.

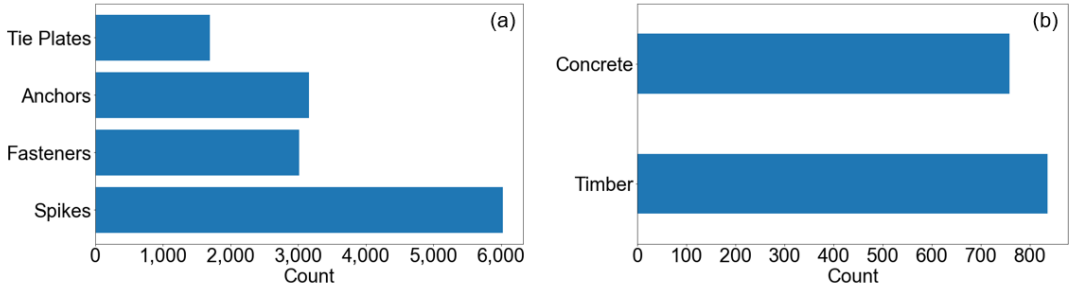

Figure 4. Example inventory of HTL Section 3 (a) number and type of hold-down devices (b) and number and type of crossties

2.4 TCHI Calculation

The TCHI Calculation takes advantage of the rail industry's familiarity with strip chart data to perform geometry data visualization (Saadat et al., 2018) to show health information about infrastructure components. First, researchers independently calculate component-level indexes for ballast (i.e., ballast health index [BHI]), crossties (i.e., crosstie health index [CHI]), and spikes and/or e-clips (i.e., fastener health index [FHI]), which are subsequently combined into a weighted index, the TCHI. The following sections provide details on TCHI calculations using example data from the HTL at TTC.

2.4.1 Ballast Health Index (BHI)

To calculate the BHI, the research team compared the height of the ballast at the crib and shoulder to the top of the crosstie. As the distance between the top of rail and top of ballast increases, the BHI value decreases. Figure 5 shows the relationship between BHI and ballast height based on business rules and method of prediction, as well as calculated BHI values for the HTL section under study.

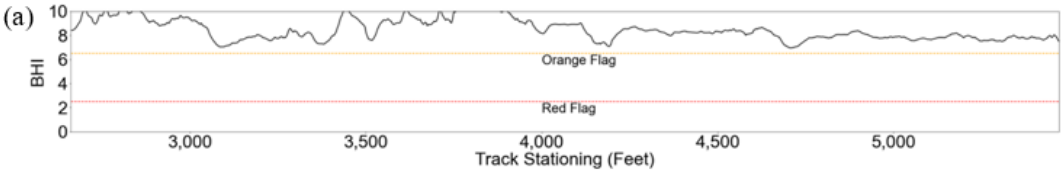

(b)

Ballast Level (in)	BHI Value	According to
≤ 8-1/16"	10	Estimation
8-1/4"	8	Estimation
8-3/8"	6.5	Compliance Threshold — Top of crosstie height
9-1/8"	6	Estimation
10-1/8"	5	Estimation
11"	3.5	Estimation
11-7/8"	2.5	Safety Threshold — Half of crosstie height
≥ 12-3/16"	0	Estimation

Figure 5. (a) Ballast data points for calculations and (b) BHI results

The colored, dashed lines represent the compliance (orange) and safety (red) thresholds of 6.5 and 2.5, respectively. Researchers considered a 33-ft moving window for all BHI calculations. Shoulder and crib ballast outputs were given equal weight when combined into a single metric, thereby lower values of BHI may be related to problems in all three sections or a single section of the ballast.

2.4.2 Crosstie Health Index (CHI)

The algorithm evaluates and grades each crosstie from zero to three, representing good, moderate, bad, and failed crossties, respectively. The first step in the CHI calculation is to count the number of crossties in each rating category for every 25-crosstie moving window in the dataset. Next, using a decision tree, researchers input these values into different equations, created based on multiple combinations of the 25 crossties with different conditions. As with BHI, UIUC established compliance and safety thresholds for the CHI. The decision tree with equations (Figure 6a), CHI output for the HTL section under study (Figure 6b), and examples from two low-scoring sections (Figure 6c) are presented to provide a visual example of the CHI methodology and results.

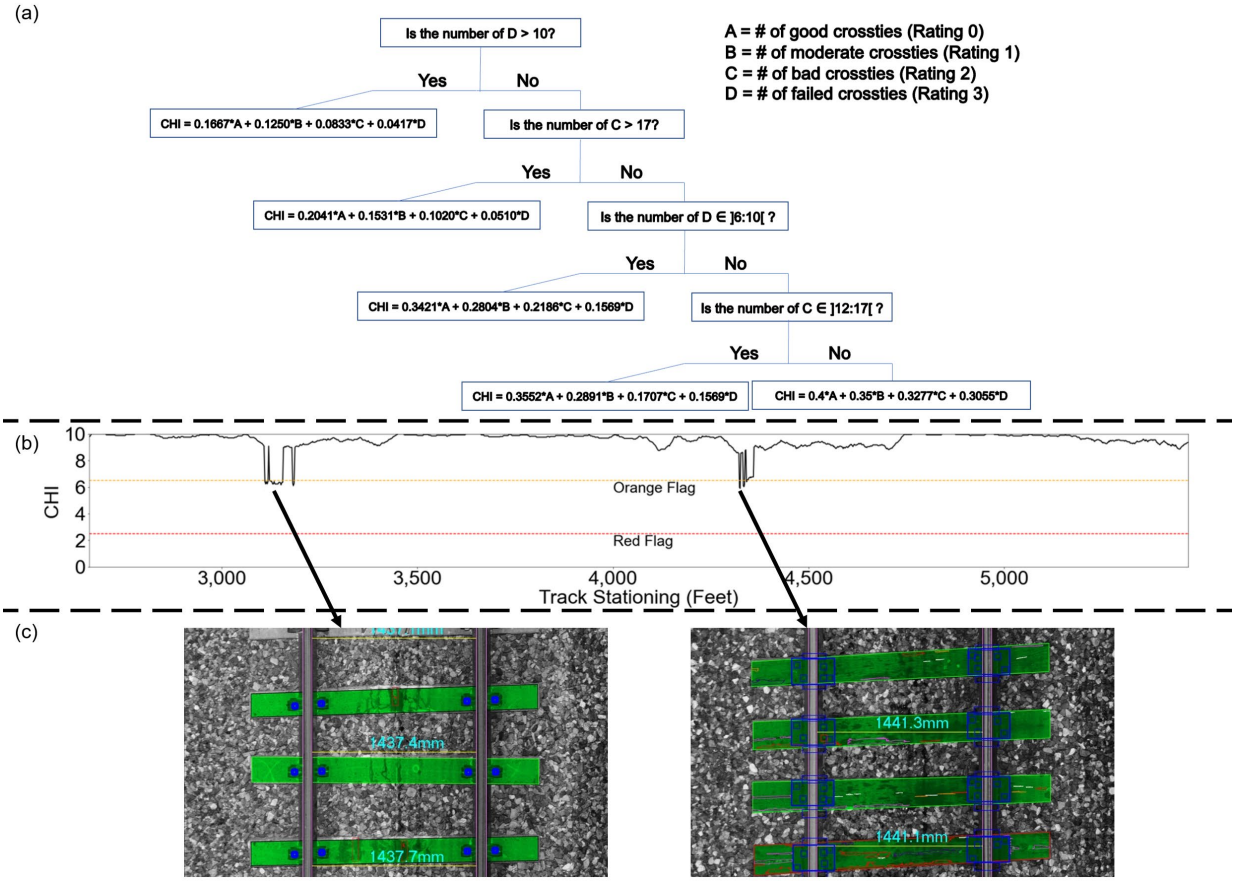

Figure 6. (a) Crosstie health index (CHI) calculation decision tree with equations, (b) results for 2,800-ft track section at HTL with two areas with lower CHI values, and (c) example concrete (left) and timber (right) cracked-crosstie image

2.4.3 *Fastener Health Index (FHI)*

The FHI is the most complex index to calculate due to the heterogeneity of fasteners, variability in how business rules are applied across the various railroads, and other differences in fastener requirements based on crosstie type. Elastic fastening system rules and calculations are used for concrete crosstie track. For timber crosstie track, two different calculations are used: one for cut and screw spikes, and another for elastic fastener systems, which combine spikes and elastic fasteners. Figure 7 shows the business rules for concrete and timber crosstie track, FHI calculations for the HTL section under study, and an example image.

(a)

Number of Fasteners in a five-crosstie window	Fastener Health Index (FHI) Value	Obtained By
20	10	Estimation
19	9	Estimation
18	8	Estimation
12	6.5	Compliance Threshold – 40% missing fasteners
10	5	Estimation
8	2.5	Safety Threshold – 60% missing fasteners
2	1	Estimation
0	0	Estimation

(b)

Number of Spikes in 25-crossties window	Fastener Health Index Value	According to
200	10	Estimation
180	8	Estimation
160	6.5	Compliance Threshold – 20% missing fasteners
140	5	Estimation
120	2.5	Safety Threshold – 40% missing fasteners
75	1.5	Estimation
40	1	Estimation
20	0	Estimation

(c)

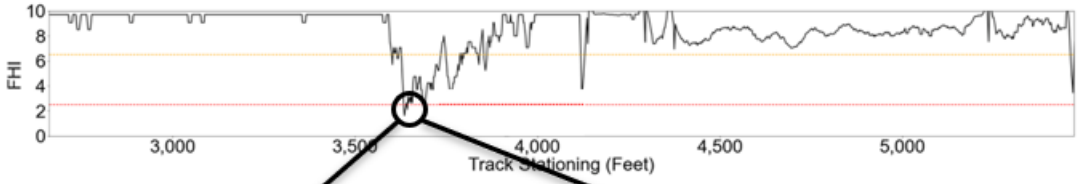

(d)

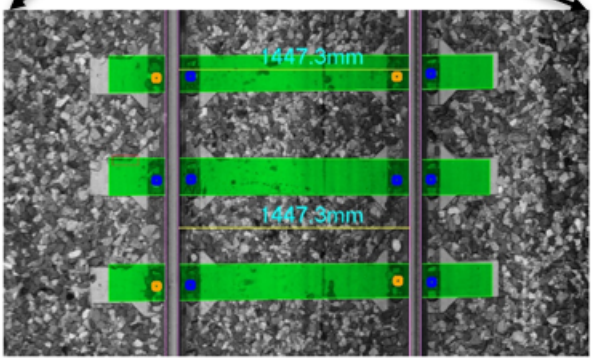

Figure 7. FHI values for (a) concrete crosstie track and for (b) timber crossties track with cut spikes, (c) FHI for results for example track section, (d) and example image result

The FHI for concrete crosstie track is based on the number of clips present in a five-crosstie moving window. Figure 7a illustrates the relationship between number of fasteners present and FHI in the window. Researchers established these relationships based on Class I business rules, research experience, and parameter estimation. For timber crosstie track (Figure 7b), the FHI for cut and screw spikes locations is based on the total number of expected spikes in a 25-crosstie window. For timber crossties with elastic fastening systems, a combination of methodologies is used to generate the FHI. The algorithm evaluates spikes within a 25-crosstie window and elastic clips within the 5-crosstie window used for concrete crossties. Researchers then apply weights to the two calculated values to determine the overall FHI for the section. A 60 percent weight is used for elastic fasteners (i.e., makes up 60 percent of the total FHI) and a 40 percent weight for spikes. The method currently does not evaluate transitions between crosstie materials due to the inherent challenges associated with boundary conditions, though rules could be developed for them in the future.

An example FHI output for the HTL (Figure 7c) indicates that the fasteners were mostly above the yellow threshold, with a subset of locations (e.g., near 3,600 and 4,150 ft) indicating lower health. Further investigation of the results between 3,600 and 3,900 revealed the presence of unique "dog-bone" crossties with a complex and non-uniform pattern of fasteners the DCNN was not trained to recognize. While the fastening systems were correctly installed, their condition was incorrectly identified as missing (false negative) due to their larger rail seat (Figure 7d).

2.4.4 Track Component Health Index

The TCHI provides a holistic view of the health of the track infrastructure based on the three track components analyzed previously (i.e., ballast, crossties, and fasteners). End-users can adjust the combination of the different sub-indexes into the TCHI based on their specific needs and business rules. In this research, UIUC assigned a greater weight (i.e., 40 percent) to the fastener components given their critical function in providing proper track gauge, while the BHI and the CHI were each responsible for 30 percent of the TCHI.

Figure 8 shows the TCHI results calculated using Equation 1 and the individual component indices as inputs for the 2,800-ft section under study. Due to the distribution of weights, the TCHI is most influenced by fastener condition (i.e., FHI) and has its lowest values at the same locations as the FHI. Nonetheless, around track station 3,200, there is a local minimum due to the combined influence of ballast level (i.e., BHI) and crosstie condition (i.e., CHI).

$$TCHI = 0.4\,FHI + 0.3\,BHI + 0.3\,CHI \qquad \text{Equation 1}$$

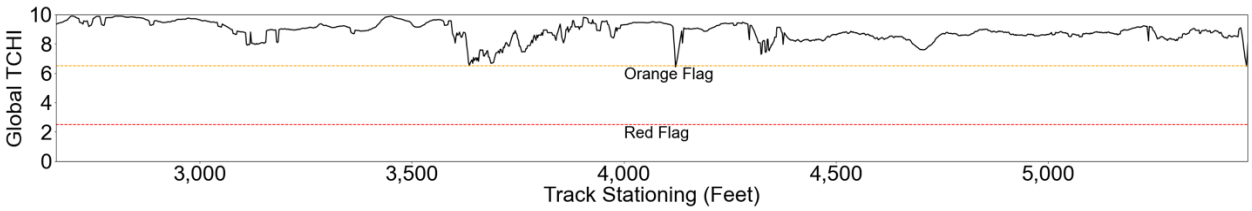

Figure 8. Example TCHI results for HTL Section 3

2.5 Summary

UIUC developed and demonstrated specific component indexes for ballast (BHI), crossties (CHI), and fasteners (FHI) that, when combined and weighted become a global track component health index (TCHI). The TCHI methodology provides an analytical and numerical way to assess track component health and holistically understand rail superstructure condition. This method can augment the functions of different stakeholders in the railway industry and serve as an effective tool to monitor and compare the state of the track as it changes over time. Results demonstrate that machine vision-based track inspections that generate linear track health and condition data can be a valuable resource for infrastructure owners. Infrastructure owners can leverage these data for the detection and tracking of condition change as a function of time and tonnage.

3. Track Strength Index (TSI) Development

This section describes a data-driven method that uses both the in-situ condition of track components and track geometry data to rate the track's lateral strength (buckling resistance). It introduces the TSI which numerically quantifies buckling resistance at a system level.

3.1 Track Strength Parameters Sensitivity Analysis

Track buckles result from the interaction of three elements: high rail compressive forces, weakened track conditions, and vehicle loads (Kish, 2003). The developed metric reflects track condition and the strength portion of buckle propensity but does not address the demand portion (i.e., rail compressive forces and train loading). UIUC researchers performed a sensitivity analysis of LR*AI*L data from CWR track using the CWR-RISK module within the software CWR-SAFE (Kish and Samavedam, 1999) to determine the major track strength parameters that influence track buckling resistance. The analysis considered several critical factors, including track curvature, crosstie-ballast friction coefficient, longitudinal stiffness, track lateral resistance, crosstie weight, misalignment amplitude, ballast type, crosstie spacing, and foundation modulus as defined by Kish and Samavedam (1999).

The researchers established a baseline (default case) using used CWR-SAFE's default track parameters: 136RE rail section, concrete crossties, granite ballast, and 5-degree curve (Kish et al., 2013). Next, researchers varied each parameter individually within the ranges defined in the software while all other parameters were held at baseline values and extracted the critical buckling temperature for each case (Figure 9).

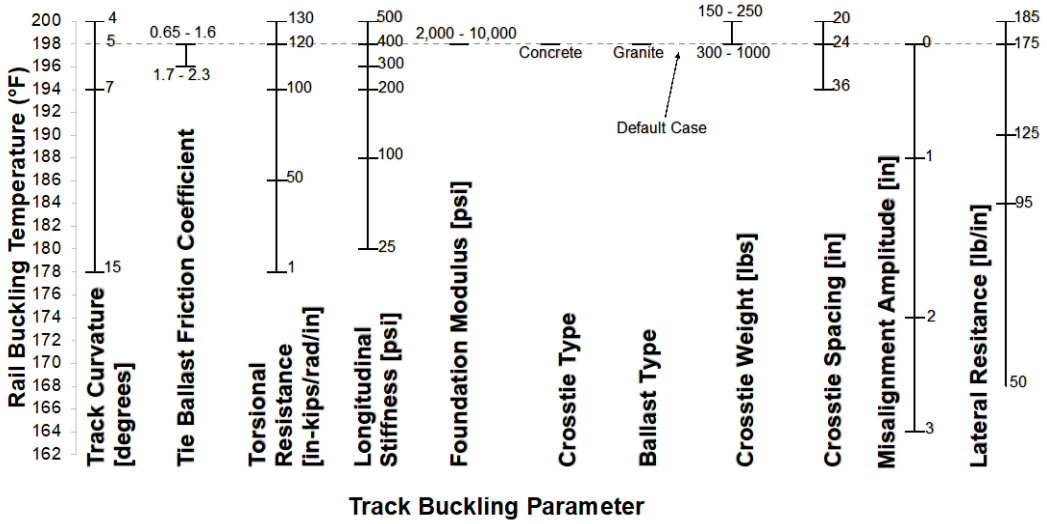

Figure 9. Sensitivity analysis of buckle risk using CWR-RISK software

The X-axis contains track features with corresponding range values shown with vertical lines. The Y-axis represents the corresponding rail buckling temperature in degrees Fahrenheit. The length of a track feature's vertical line determines the relative influence of a feature on track buckling resistance. The primary features influencing track buckling are lateral resistance, misalignment amplitude, longitudinal stiffness, torsional resistance, and track curvature. These features have substantial impact on the rail buckling temperature and, therefore, track buckling

risk. The analysis was limited to the data available from the LR*AI*L and geometry systems. The influence of torsional resistance on track buckling could not be considered in this present study, though future research should explore the influence of torsional resistance and its contribution to track buckling resistance.

3.2 TSI Parameters

The TSI calculation methodology considers misalignment amplitude, degree of curvature, longitudinal strength, and lateral strength as the primary factors contributing to buckling resistance. Track alignment and curvature are outputs from geometry car inspection data. Current moving platform inspection technology cannot quantify longitudinal and lateral strength. UIUC employed a data-driven approach for estimating lateral and longitudinal strength based on a weighted average of the condition of track components as determined by the LR*AI*L measurement system.

3.2.1 Misalignment Amplitude

Track geometry misalignment is any deviation from the design alignment of the track. Lateral misalignment quantifies the deviation of the track's actual position from its intended or desired left-to-right position. The risk of buckling increases as the size of the misalignment grows (Kish and Mui, 2003). UIUC considered a range of track misalignment from 0 to 3 inches, representing FRA alignment defect limits for track Classes 2 through 8 (FRA, 2022). The researchers performed a polynomial regression on a set of data points for misalignment amplitude values of 3, 2, 1, and 0, representing scaled values of 0, 3, 6, and 10, respectively. This resulted in Equation 2, which is used to convert misalignment values to a 0- to 10-point rating scale. The resulting misalignment score ranges from 0, representing the most significant deviation from the track's reference line (equal to or greater than 3 inches), to 10, signifying a smooth track without any alignment defects (equal to 0 inches).

$$y_1 = -0.17\,{x_1}^3 + {x_1}^2 - 4.83\,x_1 + 10 \text{ for } 0 \le x_1 \le 3 \qquad \text{Equation 2}$$

$$y_1 = 0 \text{ for } x_1 > 3$$

Here, y_1 is the scaled 10-point rating of the misalignment, and x_1 is the absolute value of maximum of left and right misalignment amplitudes. This process ensured a continuous mapping of misalignment values to the 0–10 scale, providing an assessment rate of track alignment quality.

3.2.2 Curvature

Track curvature is defined as the angular measurement between the endpoints of a specified length, typically expressed as either an arc or a chord (FRA, 2022). In North American railroad practices, the reference chord is commonly a standard length of 100 ft (Kish and Mui, 2003). Studies have shown that an increase in the degree of curvature correlates with an increase in track buckling strength (Kish et al., 2013; Zimmermann and Braess, 2017), i.e., a tangent track has greater structural integrity compared to a track with equivalent mechanical characteristics located on a curve (Zarembski and Magee, 1981). Track curvature varies depending on the specific railway standards and requirements. Small curves have curvatures ranging from 1 to 5 degrees, medium curves range from 5 degrees to 10 degrees, and sharp curves exceed 10 degrees (FRA, 2021). UIUC defined the range of curvature to be between 1 and 15 degrees. Researchers

fit a second-degree polynomial curve (Equation 3) to degree of curvature values ranging from 15 to 1 and their corresponding scaled values ranging from 0 to 10 using three assumed fixed data pairs: (15;0), (7;5), and (1;10). This allowed track curvature values to be transformed into a normalized 10-point rating scale representing the range of curvature severity.

$$y_2 = 0.015\,{x_2}^2 - 0.952\,x_1 + 10.94 \text{ for } 0 \leq x_2 \leq 15 \qquad \text{Equation 3}$$

$$y_2 = 0 \text{ for } x_2 > 15$$

In this equation, y_2 represents the scaled score of the track curvature degree, and x_2 corresponds to the track curvature degree as defined earlier.

3.2.3 Lateral Track Strength

The importance of ballast in providing sufficient strength to the track in both the lateral and longitudinal directions has been widely recognized, studied, and quantified. Studies in this area fall into two main categories. The first category focuses on the effect of ballast material properties on track lateral resistance, including ballast type, shape, density, and particle size distribution (PSD; Tutumluer et al., 2006; Fontserè et al., 2016; Sadeghi et al., 2016; Esmaeili et al., 2017; Mulhall et al., 2018; Guo et al., 2022). The second category includes ballast layer geometry parameters, particularly exploring the impact of shoulder and crib ballast dimensions on track lateral resistance (DiPilato et al., 1983; Le Pen and Powrie, 2011; Kish, 2011; Khatibi et al., 2017b; De Iorio et al., 2018; Mohammadzadeh, et al., 2018). The UIUC TSI metric is limited to ballast layer geometry properties.

There is a relatively wide range of values in the literature for the contribution of each ballast part to the total lateral resistance depending on the crosstie material, ballast material and condition, and applied vertical load. Crosstie-ballast bottom and side friction and end restraint resist the track's tendency to displace laterally (Kish and Samavedam, 2013). The bottom friction component of track resistance is primarily affected by crosstie type and weight, while crib level has the greatest influence on side friction, and ballast shoulder has the most significant impact on end restraint. In addition, ballast consolidation and compaction affects all three components to different degrees (Kish, 2011). Extensive numerical and experimental studies have been performed to characterize lateral resistance and the share each part of the ballast contributes to the total resistance. Table 5 provides a summary of field and laboratory crosstie lateral resistance values obtained from the literature.

Table 5. Studies on ballast part contribution to lateral track resistance

Reference	Percent Contribution of Each Ballast Part on Track Lateral Resistance			
	Shoulder	Crib	Base	Tie Type
(De Iorio et al., 2018)	25%	50%	25%	Concrete
(Le Pen and Powrie, 2011b)	15% to 32%	41% to 50%	28% to 35%	Concrete
(Kish, 2011)	20% to 25%	30% to 35%	35% to 40%	Not Provided
(Lichtberger, 2007)	35% to 40%	10% to 15%	45% to 50%	Not Provided
(Kish and Samavedam, 2013)	18% to 40%	20% to 27%	40% to 55%	Timber
(Samavedam et al., 1995)	10% to 20%	55% to 60%	25% to 35%	Timber
(Selig and Waters, 1994)	30% to 40%	10% to 20%	50% to 60%	Not Provided
(Mulhall et al., 2018)	15%	17%	68%	Timber
(Ngamkhanong et al., 2021)	30% to 40% 12% to 16%	20% to 34% 20% to 28%	37% to 47% 56% to 68%	Timber Concrete

The LR*AI*L system detects only what is visible from the surface. The lateral strength used in the TSI methodology is calculated based on the relative contribution of shoulder and crib ballast only and adopts the contribution percentages reported by Kish (2011). The influence of crosstie weight on increasing bottom friction and lateral strength is considered through adjustments in the upper limit of TSI and will be discussed in the following sections. Ballast level is reported as the absolute distance between a plane drawn between the top of both rails and the mean height of the ballast surface. Shoulder ballast width is measured from an offset of the rails where the crosstie ends or from a fixed 17 5/8 in between the two consecutive ties, using 4 in by 4 in bins on each side (Figure 10). Results are reported on a 3.3 ft (1 m) basis for crib, left, and right shoulder.

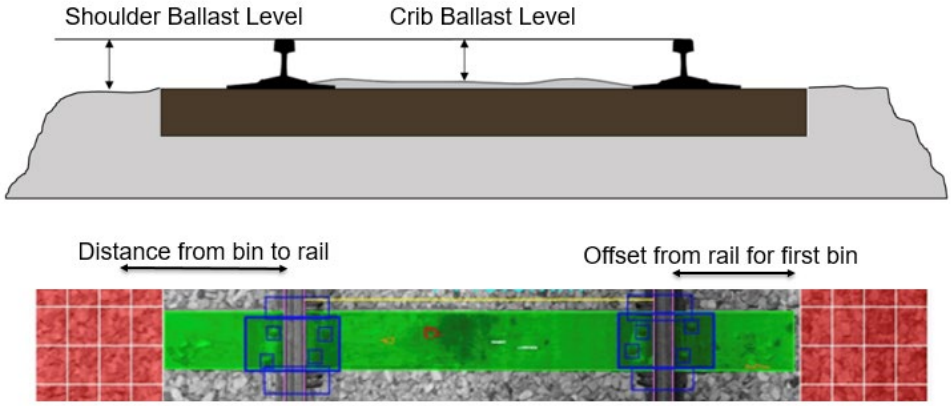

Figure 10. Ballast level (top) and width (bottom) measurement methodology

A minimum ballast shoulder width of 12 in is commonly recommended for CWR track (Hay, 1982) and is specified by most Class I railroads (BNSF Railway, 2018; Union Pacific Railroad, 2019; CSX Transportation, 2020). Studies examining various ballast levels and their impact on lateral strength have shown that ballast levels lower than top of the crosstie reduce track structural capacity and lateral resistance (Le Pen and Powrie, 2011). Therefore, UIUC assigned a rating of 10 for ballast that is even with the top of the crosstie and a rating of zero with ballast levels below the bottom of crosstie.

The first step in developing a numerical evaluation for track lateral strength based on ballast geometry properties involves comparing the existing ballast level and shoulder width to the desired values using Equation 4 and Equation 5. To convert ballast level values to a 10-point rating scale, researchers fit a linear regression to data points representing the top, half, and bottom of the crosstie (Figure 5) and their corresponding scaled values of 10, 5, and 0 in order to extract the coefficients shown in Equation 4, where y_3 represents ballast level scaled score with lower numbers corresponding to low ballast levels and x_3 is ballast level measured as the distance between top of rail and top of ballast in mm.

$$y_3 = -0.056\ x_3 + 21.94 \qquad \text{Equation 4}$$

Researchers generated Equation 5 by fitting a polynomial curve to ballast shoulder width values of 12 in (304.8 mm), 6 in (152.4 mm), and 0.8 in (20 mm), along with their corresponding scaled values of 10, 5, and 0, respectively. In Equation 5, y_4 represents shoulder width scaled score with lower numbers corresponding to narrow shoulders, and x_4 is shoulder width measured in mm.

$$y_4 = -1.7 \times 10^{-5}\ {x_3}^2 + 0.041\ x_3 - 0.81 \qquad \text{Equation 5}$$

The crib ballast score is calculated directly using Equation 4, while the shoulder ballast score is composed of the shoulder ballast level and width scores obtained from Equation 4 and Equation 5. Since low ballast shoulders result in larger lateral resistance reduction compared to full shoulders, shoulder ballast scores are weighted by two when combined with crib ballast score into a single value. Given the higher relative importance of shoulder ballast on the high side of a curve, shoulder ballast is considered a weighted average of high and low sides in curved track, with a ratio of 2:1. Conversely, both are weighted equally (1:1) in tangent track. The lateral strength index is calculated as a weighted average of the shoulder and crib ballast scores where the weight ratio of crib to shoulder ballast is 1.5, which is based on the contribution percentages reported by Kish et al. (2011). The overall lateral strength is also reported using a scale of 0 to 10.

3.2.4 Longitudinal Track Strength

Crossties, ballast, and fastening systems and their collective interaction with the rails provide track longitudinal resistance. Rails move in the longitudinal direction due to thermal force gradients and train traction demands (Samavedam et al., 1993). The fastening system connects the rail to the crossties. When crossties are unanchored or loosely anchored, track longitudinal resistance is minimal. When crossties are securely anchored, the ballast provides significant longitudinal resistance. Table 6 provides a summary of literature quantifying the contributions of the crib, shoulder, and support ballast to overall track longitudinal resistance.

Table 6. Studies on ballast part contribution to longitudinal track resistance

Reference	Percent Contribution of Each Ballast Part on Track Longitudinal Resistance			
	Shoulder	Crib	Base	Tie Type
(Dersch et al., 2023b)	0% to 10%	60% to 75%	25% to 40%	Timber Concrete
(Zakeri and Yousefian, 2020)	12%	67%	21%	Concrete
(De Iorio et al., 2018b)	13%	59%	28%	Concrete
(ERRI, 1997)	13%	51%	36%	Not Provided

The TSI uses the relative contribution of shoulder and crib ballast and considers the crosstie bottom friction via crosstie type. The contribution of shoulder ballast on longitudinal strength is low and not considered in the TSI calculations. Researchers defined longitudinal strength as a weighted average of crib ballast level and tie anchoring pattern at a ratio of 4:1. Equation 4 is used for converting crib ballast level to the 10-point rating scale. The anchorage pattern is rated based on its influence on resisting track movement. Assigned scores were out of 10 for concrete tie with elastic fastener, 8 for track with every tie anchored, and 6 for track with every other tie anchored. The overall longitudinal strength is also reported using a scale of 0 to 10.

3.2.5 Crosstie Type

TSI calculations considered crosstie type due to its contribution to both lateral and longitudinal resistance. As the crosstie bottom roughness increases, lateral and longitudinal track resistance increases as ballast particles lock into the surface irregularities (Samavedam et al., 1993). Timber crossties allow for more ballast interlock than concrete crossties. Concrete crossties produce higher frictional forces between tie and ballast than timber ties due to their higher mass and larger contact area. The TSI metric assumes that concrete crossties are stronger laterally than timber crossties. Crosstie weight is the primary contributor to the lateral resistance in the elastic zone (the zone of interest for buckling), and once slip occurs, the friction plays the primary role

(Zimmermann and Braess, 2017). To reflect this, the TSI sets 9 as the maximum value for timber track and 10 for concrete track. This is consistent with test results summarized by Zarembski (2016) in which lateral resistance of a concrete crosstie is greater than the resistance offered by a timber crosstie by a factor of 1.2 and 1.3 for strong and weak track, respectively. Similar differences are observed between timber and concrete crossties with respect to their longitudinal resistance.

3.3 Track Strength Index (TSI)

The TSI methodology is based on a weighted calculation approach that applies weights to each factor based on its influence on the overall track strength in terms of buckling resistance, with a special emphasis on ballast levels and configurations. The methodology combines the four parameters defined earlier to produce a numerical value for track strength in terms of buckling resistance (Equation 6).

$$TSI = \frac{\sum(w_i \cdot f_i)}{\sum(w_i)} \qquad \text{Equation 6}$$

f_i represents each factor (i ranging from 1 to 4 corresponding to misalignment amplitude, curvature, lateral strength, and longitudinal strength respectively), and w_i is the assigned weight for each factor.

Table 7 provides a summary of all included factors and their defined ranges. After calculating each factor and converting it to the corresponding 9- or 10-point scale for concrete and timber crosstie track, respectively, the TSI is calculated by applying the weights shown in Table 7 to each factor and is reported for each analyzed track section indicating the buckling resistance. Higher values represent a stronger track in terms of buckling resistance.

Table 7. TSI input variables, ranges, scaled values, and weights

i	Factor	Range & Score	Weight
1	Misalignment Amplitude	0" = 10 3" = 0	3
2	Degree of Curvature	0° = 10 15° = 0	2
3	Longitudinal Strength		
	Fastening/Anchorage Pattern	CTEF = 10 ETA = 8 EOTA = 6	6
	Crib Ballast Level	Top of Tie = 10 Half Tie Height = 5 Bottom of Tie = 0	
4	Lateral Strength		
	Shoulder Ballast Level	Top of Tie = 10 Half Tie Height = 5 Bottom of Tie = 0	9
	Shoulder Ballast Width	12" = 10 0" = 0	

The parameter weights are defined to best represent track conditions of interest. Ballast has consistently been identified to be a critical component in providing adequate lateral and longitudinal track strength and is of great importance in track buckling investigation. To

demonstrate the influence of ballast on the TSI, researchers studied different revenue service scenarios (Figure 11). Each scenario represents a unique ballast configuration. The corresponding TSI calculation assumes all other parameters shown in Table 7 are at their maximum values to provide a uniform baseline for comparison. Empty cribs have the most significant impact on TSI reduction, followed by the scenario where both shoulders are missing. That is because the crib ballast contributes to both lateral and longitudinal resistance while shoulder ballast only impacts lateral strength.

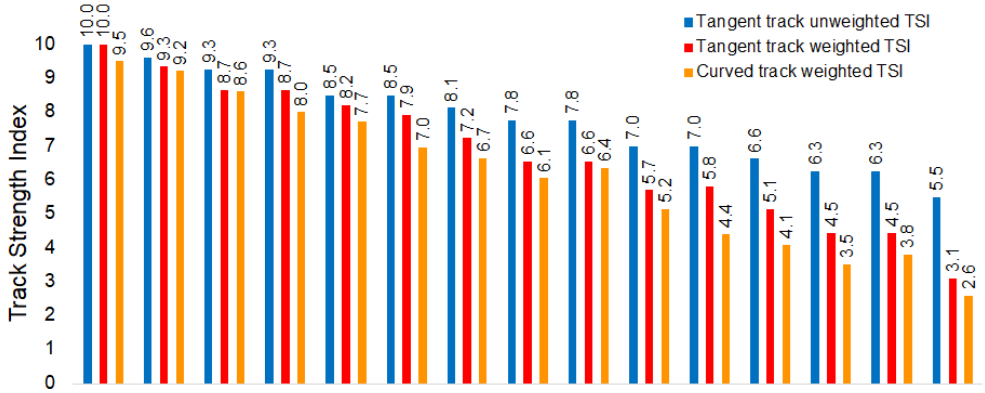

Ballast Configuration	1	2	3	4	5	6	7	8	9	10	11	12	13	14	15
Crib	F	F	F	F	F	H	H	H	H	H	E	E	E	E	E
Left Shoulder	F	F	H	F	E	F	F	H	F	E	F	F	H	F	E
Right Shoulder	F	H	H	E	E	F	H	H	E	E	F	H	H	E	E

F = Full; H = Half; E = Empty

Figure 11. Summary of weighted and unweighted TSI values

Figure 11 reveals that the unweighted TSI does not adequately reflect the track strength in cases where ballast is missing from parts of the track. For instance, in skeletonized tracks, the unweighted index value is 5.5, while the weighted index is 3.1. It is important to note that while skeletonized track lacks much of the frictional component of resistance, it does retain minimal resistance due to the performance of the track as a system. Railroads could define thresholds internally to better interpret TSI by flagging the locations where the index does not meet the required track strength.

Figure 12 (top) shows the 10-point scaled output of the TSI along a section of track using a strip chart. The vertical axis represents the index value while the horizontal axis represents the distance along the track (e.g., milepost location). UIUC tested the TSI metric using revenue service data collected from a Class I railroad. The subdivision includes tangent and curved track and has both timber and concrete crosstie sections. The number of concrete crossties is less than half of timber. Figure 12 (top) shows the TSI for a sample 3-mile section of the 107-mile test corridor. Although no exceptional condition is observed, there are variations in TSI results that are related to the variability in crosstie materials (i.e., concrete interspersed with timber). Moreover, larger dips in the TSI results are observed around mile 2.6. As illustrated in Figure 12 (middle), low shoulder ballast levels (defined as 6.1 inches below top-of-crosstie and identified by the red shaded areas) are present in this region. To validate this case, Figure 12 (bottom) presents the ballast geometry cross section along with the design cross section and illustrates low shoulder ballast on both sides. This comparison also allows users to quantify the volume of

missing ballast benefiting maintenance planning. In addition to the low ballast levels, some skewed crossties are present, indicating low resistance to crosstie movement.

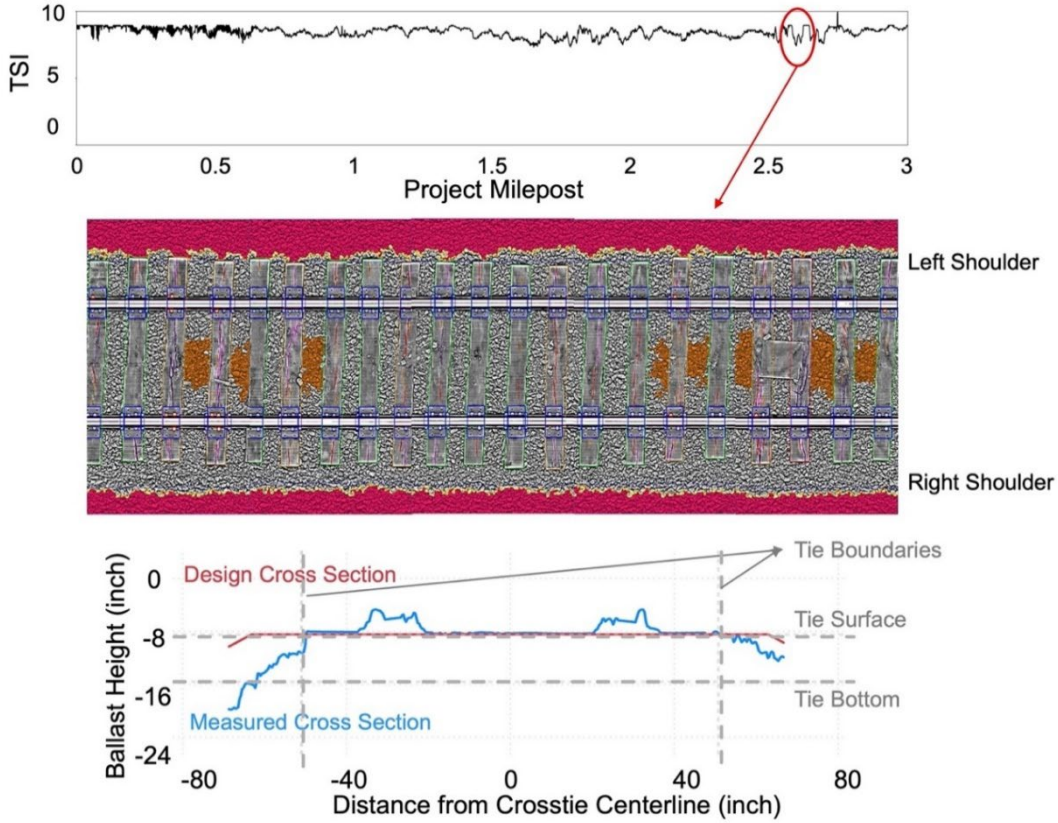

Figure 12. Strip chart of TSI results for sample section (top), marked-up 2D intensity images of the track at mile 2.6 showing low shoulder ballast levels (middle), ballast cross section details of the track at mile 2.6 (bottom)

3.4 Summary

The sensitivity analysis conducted using CWR-Risk identified misalignment amplitude, track curvature, lateral resistance, and longitudinal resistance as key factors affecting buckling resistance. Torsional resistance was excluded due to data limitations. UIUC developed a metric using mathematical tools to convert track feature data into 10-point scales that were combined through weighted averaging into a TSI to quantify track strength to withstand buckling forces. Evaluating 15 ballast scenarios revealed the significant impact of empty cribs and absent shoulders on track strength. Crib ballast affects lateral and longitudinal resistance, while shoulder ballast influences only lateral strength. Further, TSI results from a sample section of a test corridor demonstrated that the methodology could identify areas of diminished track strength (e.g., low shoulder ballast) and help infrastructure owners better identify higher-risk areas and target maintenance.

4. Conclusion

The objective of this project was to develop new methodologies and indexes to consume outputs from the LR*AI*L inspections system to enable a more complete understanding of track condition. UIUC developed a system of track component health indices from LR*AI*L track inspection data. The research team developed and demonstrated specific component indexes for ballast, crossties, and fasteners and a combined and weighted overall track component health index (TCHI). At a system level, researchers developed a new global index, the track strength index (TSI) to numerically assess the track strength with a focus on track buckle resistance. The methodology was intentionally developed to be technology-agnostic given the rapid development and deployment of sensing devices for the railroad industry. Thus, the methodology can be used with data from other inspection systems that output similar track component conditions. From this study, the following findings and conclusions are drawn:

- The TCHI methodology provides an analytical and numerical way to assess track component health and holistically understand track superstructure condition. This method can augment the functions of different stakeholders in the railway industry and serve as an effective tool to monitor and compare the state of the track as it changes over time.
- Results demonstrate that machine vision-based track inspections that generate linear track health and condition data can be a valuable resource for infrastructure owners. Users can leverage these data for the detection and trending of condition change as a function of time and tonnage.
- Methods for visualization of data that were developed and demonstrated in this study can aid decision-makers in their prioritization and optimization of maintenance strategies to further mitigate of risk of track caused derailments. With recurring gathering, storage, and dissemination of these data, additional analytics may be developed for predictive maintenance and capital planning forecasting.
- A sensitivity analysis conducted using CWR-Risk software identified misalignment amplitude, track curvature, lateral resistance, crosstie torsional resistance, and longitudinal resistance as the primary factors contributing to buckling resistance.
- The most notable effect on TSI reduction occurs when crib ballast is low, and the second most impactful scenario is when both shoulders have low ballast levels.

Employing owner-specific business rules or engineering requirements could be used to achieve further refinement of TCHIs and their sub-indices, resulting in more reliable and accurate assessment of infrastructure. The nature of the LR*AI*L and the DCNNs employed allows the system to identify new components and be re-trained when new data are collected, further improving system accuracy and precision. In addition, future work should focus on developing an alternative (and comprehensive) model or index that considers the demand side of track buckle equation. This new index should incorporate rail temperature, its deviation from RNT, and forces induced by trains accelerating and braking. By employing more advanced computational approaches, both sides of the buckling equation can be integrated, thereby leading to a more comprehensive assessment considering capacity and demand. The results for such an improved model should also undergo revenue service field validation and benchmarking against currently available models for track strength and propensity to buckling.

References

Andersson, M. (2002). *Strategic Planning Of Track Maintenance*. KTH Royal Institute of Technology, Borlänge, Sweden.

Association of American Railroads (2020). *Annual Report Of Hazardous Materials Transported By Rail*. BOE 20-1.

Belding, M., Enshaeian, A., & Rizzo, P. (2023). Nondestructive rail neutral temperature estimation based on low-frequency vibrations and machine learning. *NDT & E International*, 137: 102840 DOI: 10.1016/j.ndteint.2023.102840.

BNSF Railway, E.S. (2018). *Guidelines For Industry Track Projects*. BNSF Railway Company. Kansas City, KS.

Clark, R. (2004). Rail Flaw Detection: Overview and Needs for Future Developments. *NDT & E International*, 37(2): 111–118 DOI: 10.1016/j.ndteint.2003.06.002.

CSX Transportation (2020). *Engineering Department Maintenance Of Way Field Manual*. CSX Transportation, Jacksonville, Florida.

De Iorio, A., Grasso, M., Penta, F., Pucillo, G.P., Rossi, S., & Testa, M. (2018). On the ballast–sleeper interaction in the longitudinal and lateral directions. *Proceedings of the Institution of Mechanical Engineers, Part F: Journal of Rail and Rapid Transit*, 232(2): 620–631 DOI: 10.1177/0954409716682629.

Dersch, M., Roadcap, T., Edwards, J.R., Qian, Y., Kim, J.-Y., & Trizotto, M. (2019). Investigation into the Effect of Lateral and Longitudinal Loads on Railroad Spike Stress Magnitude and Location Using Finite Element Analysis. *Engineering Failure Analysis*, 104: 388–398 DOI: 10.1016/j.engfailanal.2019.06.009.

Dersch, M.S., Potvin, M., De O. Lima, A., & Edwards, J.R. (2023a). Effect of Critical Factors Influencing Longitudinal Track Resistance Leveraging Field Experimentation. *Transportation Research Record: Journal of the Transportation Research Board*,: 03611981231187641 DOI: 10.1177/03611981231187641.

Dersch, M.S., Potvin, M., De O. Lima, A., & Edwards, J.R. (2023b). Effect of Critical Factors Influencing Longitudinal Track Resistance Leveraging Laboratory Track Panel Pull Test Experimentation. *Transportation Research Record: Journal of the Transportation Research Board*.

DiPilato, M.A., Steinberg, E.I., & Simon, R.M. (1983). *Ballast And Subgrade Requirements Study*.

Ebersohn, W., & Ruppert, C. (1998). Implementing a railway infrastructure maintenance system. Central Queensland University, Rockhampton, Queensland, Australia.

Esmaeili, M., Nouri, R., & Yousefian, K. (2017). Experimental comparison of the lateral resistance of tracks with steel slag ballast and limestone ballast materials. *Proceedings of the Institution of Mechanical Engineers, Part F: Journal of Rail and Rapid Transit*, 231(2): 175–184 DOI: 10.1177/0954409715623577.

Evani, S.K., Spalvier, A., & Popovics, J.S. (2021). Air-Coupled Ultrasonic Assessment of Concrete Rail Ties. *NDT & E International*, 123: 102511 DOI: 10.1016/j.ndteint.2021.102511.

Federal Railroad Administration (2017). Chapter 1 - Track Safety Standards, Classes 1 Through 5, In: *Track and Rail Infrastructure Integrity Compliance Manual*. US Department of Transportation, Federal Railroad Administration, Washington, DC, USA. pp.189.

Federal Railroad Administration (2011). Part 213 - Track Safety Standards, In: *Title 49 of the Code of Federal Registrations*. US Department of Transportation, Federal Railroad Administration, Washington, DC, USA. pp.100–154.

Fontserè, V., Pita, A.L., Manzo, N., & Ausilio, A. (2016). NEOBALLAST: New High-performance and Long-lasting Ballast for Sustainable Railway Infrastructures. *Transportation Research Procedia*, 14: 1847–1854 DOI: 10.1016/j.trpro.2016.05.151.

Fox-Ivey, R., Nguyen, T., & Laurent, J. (2020a). *Laser Triangulation For Track Change And Defect Detection*. Federal Railroad Administration, Office of Research, Development and Technology, DOT/FRA/ORD-20/08. Washington, D.C., USA.

Fox-Ivey, R., Nguyen, T., & Laurent, J. (2020b). *Extended Field Trials Of LRAIL For Automated Track Change Detection*. Federal Railroad Administration, Office of Research, Development and Technology, DOT/FRA/ORD-20/14. Washington, D.C., USA.

FRA (2020). *Field Orientation Training Guide – Track Discipline*. US Department of Transportation, Federal Railroad Administration. Washington, DC, USA.

FRA (2021). FRA Guidance on Continuous Welded Rail (CWR) Plan Requirement - Background and Example Generic Plan.

FRA (2022). Part 213 - Track Safety Standards, In: *Title 49 of the Code of Federal Registrations*. US Department of Transportation, Federal Railroad Administration, Washington, DC, USA. pp.100–154.

Gao, Y., Miller, M., & Williams, D. (2020). *Field Investigation Of Broken Cut Spikes On Elastic Fastener Plates: Revenue Service*. TTCI, Technology Digest, TD20-013. Pueblo, CO, USA.

Guo, Y., Xie, J., Fan, Z., Markine, V., Connolly, D.P., & Jing, G. (2022). Railway ballast material selection and evaluation: A review. *Construction and Building Materials*, 344: 128218 DOI: 10.1016/j.conbuildmat.2022.128218.

Harrington, R., Edwards, J.R., de O. Lima, A., Dersch, M.S., Fox-Ivey, R., Laurent, J., & Nguyen, T. (2022). Use of Deep Convolutional Neural Networks (DCNNs) and Change Detection Technology for Railway Track Inspections. *Proceedings of the Institution of Mechanical Engineers, Part F: Journal of Rail and Rapid Transit*,: 1–9.

Harrington, R.M., de O. Lima, A., Edwards, J.R., Dersch, M.S., Fox-Ivey, R., Laurent, J., & Nguyen, T. (2023). *Automated Track Change Detection Technology For Enhanced Railroad Safety Assessment*. 0704–0188. Washington DC, USA.

Hasan, N. (2021). Buckling of a ballasted curved track under unloaded conditions. *Advances in Mechanical Engineering*, 13(6): 16878140211025187 DOI: 10.1177/16878140211025187.

Hasap, A., Paitekul, P., Noraphaiphipaksa, N., & Kanchanomai, C. (2018). Analysis of the fatigue performance of elastic rail clip. *Engineering Failure Analysis*, 92: 195–204 DOI: 10.1016/j.engfailanal.2018.05.013.

Hay, W.W. (1982). *Railroad Engineering*, Second ed. John Wiley & Sons, New York, NY, USA.

Huang, H., Tutumluer, E., & Dombrow, W. (2009). Laboratory characterization of fouled railroad ballast behavior. *Transportation Research Record: Journal of the Transportation Research Board*, 2117: 93–101 DOI: 10.3141/2117-12.

Kerr, A.D. (2003). *Fundamentals Of Railway Track Engineering*. Simmons Boardman, Omaha, NE, USA.

Khatibi, F., Esmaeili, M., & Mohammadzadeh, S. (2017a). DEM analysis of railway track lateral resistance. *Soils and Foundations*, 57(4): 587–602 DOI: 10.1016/j.sandf.2017.04.001.

Khatibi, F., Esmaeili, M., & Mohammadzadeh, S. (2017b). DEM analysis of railway track lateral resistance. *Soils and Foundations*, 57(4): 587–602 DOI: 10.1016/j.sandf.2017.04.001.

Kish, A. (2003). *Track Buckling Research*. US Department of Transportation's Volpe Center, dot_11985.

Kish, A. (2011). On the Fundamentals of Track Lateral Resistance. The American Railway Engineering and Maintenance-of-Way Association, Chicago, IL, USA, pp. 45.

Kish, A., & Mui, W. (2003). Track buckling researchJohn A. Volpe National Transportation Systems Center (U.S.), (Ed.) .

Kish, A., & Samavedam, G. (1999). RISK ANALYSIS BASED CWR TRACK BUCKLING SAFETY EVALUATIONS.

Kish, A., & Samavedam, G. (2013). *Track Buckling Prevention: Theory, Safety Concepts, And Applications*. John A. Volpe National Transportation Center.

Kish, A., Samavedam, G., & Volpe National Transportation Systems Center (2013). *Track Buckling Prevention : Theory, Safety Concepts, And Applications*. DOT/FRA/ORD-13/16.

Le Pen, Powrie, L.M. and W. (2011). Contribution of Base, Crib, and Shoulder Ballast to the Lateral Sliding Resistance of Railway Track: A Geotechnical Perspective. *Proceedings of the Institution of Mechanical Engineers, Part F: Journal of Rail and Rapid Transit*, 225(2): 113–128 DOI: 10.1177/0954409710397094.

Liu, R.-K., Xu, P., Sun, Z.-Z., Zou, C., & Sun, Q.-X. (2015). Establishment of Track Quality Index standard recommendations for Beijing Metro. *Discrete Dynamics in Nature and Society*, 2015: 1–9 DOI: 10.1155/2015/473830.

Lovett, A.H., Dick, C.T., & Barkan, C.P.L. (2015). Determining Freight Train Delay Costs on Railroad Lines in North America. , Tokyo, Japan.

Maal, L., & Carr, G.A. (2011). *Effect Of Missing Or Broken Fasteners On Gage Restraint Of Concrete Ties*. Research Results, RR11-18. Washington, DC, USA.

Moaveni, M., Qian, Y., Qamhia, I.I.A., Tutumluer, E., Basye, C., & Li, D. (2016). Morphological Characterization of Railroad Ballast Degradation Trends in the Field and Laboratory. *Transportation Research Record*, 2545(1): 89–99 DOI: 10.3141/2545-10.

Mohammadzadeh, S., Esmaeili, M., & Khatibi, F. (2018). A new field investigation on the lateral and longitudinal resistance of ballasted track. *Proceedings of the Institution of Mechanical Engineers, Part F: Journal of Rail and Rapid Transit*, 232(8): 2138–2148 DOI: 10.1177/0954409718764190.

Mulhall, C., Balideh, S., Macciotta, R., Hendry, M., Martin, D., & Edwards, T. (2018). Large-Scale Laboratory Testing of the Lateral Resistance of a Timber Tie. In: *Railroad Ballast Testing And Properties*, ASTM International, pp. 216–236.

Ngamkhanong, C., Feng, B., Tutumluer, E., Hashash, Y. M.A., & Kaewunruen, S. (2021). Evaluation of lateral stability of railway tracks due to ballast degradation. *Construction and Building Materials*, 278: 122342 DOI: 10.1016/j.conbuildmat.2021.122342.

Potvin, M., Dersch, M., & Edwards, J.R. (2023). Review of Critical Factors Influencing Longitudinal Track Resistance. *Transportation Research Record: Journal of the Transportation Research Board*, 2677(7): 558–569 DOI: https://doi.org/10.1177/03611981231155170.

Rudy, J., Al-Qadi, I., Boyle, J., Roberts, R., & Tutumluer, E. (2006). Railroad Ballast Fouling Detection Using Ground Penetrating Radar – A New Approach Based on Scattering from Voids. , Berlin, Germany, pp. 8.

Saadat, S., Sherrock, E., & Zahaczewski, J. (2018). *Autonomous Track Geometry Measurement Technology Design, Development, And Testing*. Department of Transportation, Federal Railroad Administration. Washington, DC, USA.

Sadeghi, J., & Askarinejad, H. (2010). Development of improved railway track degradation models. *Structure and Infrastructure Engineering*, 6(6): 675–688 DOI: 10.1080/15732470801902436.

Sadeghi, J., Motieyan-Najar, M.E., Zakeri, J.A., Yousefi, B., & Mollazadeh, M. (2018). Improvement of railway ballast maintenance approach, incorporating ballast geometry and fouling conditions. *Journal of Applied Geophysics*, 151: 263–273 DOI: 10.1016/j.jappgeo.2018.02.020.

Sadeghi, J.M., Zakeri, J.A., & Najar, M.E.M. (2016). Developing Track Ballast Characteristic Guideline In Order To Evaluate Its Performance. *International Journal of Railway*, 9(2): 27–35 DOI: 10.7782/IJR.2016.9.2.027.

Samavedam, G., Kish, A., Purple, A., & Schoengart, J. (1993). *Parametric Analysis And Safety Concepts Of CWR Track Buckling*. FRA.

Sogin, S.L., Barkan, C.P.L., Lai, Y.-C., & Saat, M.R. (2012). Measuring the Impact of Additional Rail Traffic Using Highway and Railroad Metrics. In: *2012 Joint Rail Conference*, American Society of Mechanical Engineers, Philadelphia, Pennsylvania, USA, pp. 475–484.

Soleimanmeigouni, I., Ahmadi, A., Khajehei, H., & Nissen, A. (2020). Investigation of the effect of the inspection intervals on the track geometry condition. *Structure and Infrastructure Engineering*, 16(8): 1138–1146 DOI: 10.1080/15732479.2019.1687528.

Tesic, P., Jovanovic, S., & Dick, M. (2018). Analysis of vehicle/track interaction measurement data using the V/TI Monitor system. *Gradjevinar*, 70: 105–119 DOI: 10.14256/JCE.2067.2017.

Tutumluer, E., Huang, H., & Hashash, Y. (2006). Aggregate Shape Effects on Ballast Tamping and Railroad Track Lateral Stability.

Union Pacific Railroad (2019). *Engineering Track Maintenance - Field Handbook*. Union Pacific Railroad, Omaha, NE.

Van, M.A. (1996). Buckling Analysis of Continuous Welded Rail Track. *Journal of Heron*, 41(3): 175–186.

Wang, B., & Barkan, C.P.L. (2017). Principal Factors Contributing to Heavy Haul Freight Train Safety Improvements in North America: A Quantitative Analysis. , Cape Town, South Africa, pp. 67–71.

Wu, Y., Zhu, X., Huang, C.-L., Lee, S., Dersch M., & Popovics, J.S. (2021). Rail Neutral Temperature Estimation Using Field Data, Numerical Models, and Machine Learning. In: *2021 Joint Rail Conference*, American Society of Mechanical Engineers, Virtual, Online, pp. V001T12A001.

Yan, T.-H., & Corman, F. (2020). Assessing and Extending Track Quality Index for Novel Measurement Techniques in Railway Systems. *Transportation Research Record: Journal of the Transportation Research Board*, 2674(8): 24–36 DOI: 10.1177/0361198120923661.

Ying Li, Trinh, H., Haas, N., Otto, C., & Pankanti, S. (2014). Rail Component Detection, Optimization, and Assessment for Automatic Rail Track Inspection. *IEEE Transactions on Intelligent Transportation Systems*, 15(2): 760–770 DOI: 10.1109/TITS.2013.2287155.

Zarembski, A.M. (2016). Survey of Techniques and Approaches for Increasing the Lateral Resistance of Wood Tie Track.

Zarembski, A.M., & Magee, G.M. (1981). An Investigation of Railroad Maintenance Practices to Prevent Track Buckling.

Zimmermann, M., & Braess, H.P. (2017). Modelling of curve breathing in tight curves. : 9 p. DOI: 10.3929/ETHZ-B-000180683.

Abbreviations and Acronyms

ACRONYM	DEFINITION
BHI	Ballast Health Index
CHI	Crosstie Health Index
CSV	Comma Separated Values
CWR	Continuous Welded Rail
DCNN	Deep Convolutional Neural Network
FHI	Fastener Health Index
FRA	Federal Railroad Administration
HTL	High Tonnage Loop
RailTEC	Rail Transportation Engineering Center
RNT	Rail Neutral Temperature
TCHI	Track Component Health Index
TSI	Track Strength Index
TTC	Transportation Technology Center
UIUC	University of Illinois at Urbana-Champaign
VTI	Vehicle-Track Interaction